

# Magnetic excitations in NpCoGa<sub>5</sub>

N. Magnani,<sup>1</sup> A. Hiess,<sup>2</sup> R. Caciuffo,<sup>1</sup> E. Colineau,<sup>1</sup> F. Wastin,<sup>1</sup> J. Rebizant,<sup>1</sup> and G. H. Lander<sup>1</sup>

<sup>1</sup>*European Commission, Joint Research Centre, Institute for Transuranium Elements, Postfach 2340, D-76125 Karlsruhe, Germany*

<sup>2</sup>*Institut Laue Langevin, BP 156, F-38042 Grenoble Cedex 9, France*

(Dated: February 1, 2008)

We report the results of inelastic neutron scattering experiments on NpCoGa<sub>5</sub>, an isostructural analogue of the PuCoGa<sub>5</sub> superconductor. Two energy scales characterize the magnetic response in the antiferromagnetic phase. One is related to a non-dispersive excitation between two crystal field levels. The other at lower energies corresponds to dispersive fluctuations emanating from the magnetic zone center. The fluctuations persist in the paramagnetic phase also, although weaker in intensity. This supports the possibility that magnetic fluctuations are present in PuCoGa<sub>5</sub>, where unconventional *d*-wave superconductivity is achieved in the absence of magnetic order.

PACS numbers: 71.27.+a; 75.30.-m; 78.70.Nx; 75.30.Et

Many complex and diverse phenomena have been observed in the series of isostructural RTX<sub>5</sub> intermetallic compounds containing cerium or a light actinide element R, a transition metal T (Fe, Co, Ni, Rh, Ir), and an element of the boron group X (Ga or In). Current research on this family is enhanced by the possibility to explore links between unconventional superconductivity, magnetism, and non-Fermi liquid behavior in proximity of a quantum critical point [1]. Especially the discovery of *d*-wave superconductivity in PuCoGa<sub>5</sub> at the surprisingly high critical temperature of  $T_{sc} = 18$  K [2] raised much interest. No long-range magnetic order is observed in PuCoGa<sub>5</sub>, but theoretical work [3, 4, 6?] as well as recent NMR experiments [7] suggest the presence of spin polarization and hence strong magnetic correlations. Evidence for non *s*-wave superconductivity is reported also for CeRhIn<sub>5</sub> and CeCoIn<sub>5</sub>, where heavy fermion character is consistent with proximity to magnetic order [1].

Although magnetic fluctuations have been proposed to stabilize superconductivity for both Pu and Ce-based compounds, no direct measurement of magnetic fluctuation spectra has yet been reported. This is mainly because of the large neutron absorption cross-section of <sup>239</sup>Pu and <sup>113</sup>In, and the lack of large single crystals of <sup>242</sup>PuCoGa<sub>5</sub>. Thus, at present, there is no information on the electronic excitations in this interesting set of materials.

Here we present the results of inelastic neutron scattering (INS) experiments on the neptunium-based analogue NpCoGa<sub>5</sub>. This compound (space group P4/mmm,  $a = 4.277$  Å,  $c = 6.787$  Å) shows antiferromagnetic (AF) order below  $T_N = 47$  K, with an ordered Np moment  $\mu = 0.84\mu_B$  [8] pointing along the tetragonal *c*-axis [9]. The magnetic structure is defined by the propagation vector (0 0 1/2). This is exactly the reciprocal space position where theory predicts the dominant weight for the magnetic fluctuations in PuCoGa<sub>5</sub> [6]. We therefore expect some similarities between the latter and the magnetic excitations in the antiferromagnetic compound NpCoGa<sub>5</sub>.

For this experiment we used a large single crystal with a mass of 1.1 g, grown and characterized at the Institute for Transuranium Elements, Karlsruhe. Measurements were performed with the thermal triple axis spectrometer IN8 at the Institut Laue-Langevin, Grenoble, using a Si(1 1 1) focussing monochromator, open collimation, two graphite filter for second-order contamination suppression, and a pyrolytic graphite (0 0 2) analyzer.

The final wave-vector was fixed at  $k_f = 2.662$  Å<sup>-1</sup>. The crystal was oriented with the *a*- and *c*-axis in the scattering plane. Several structural Bragg peaks were measured to test its quality, found to be adequate for an INS experiment. The rocking curve ( $\Theta$  sample rotation) at the (0 0 3) Bragg reflection shows a double-peak structure, the two maxima being separated by about 1.6 degrees and each peak having 0.9 degrees full width at half maximum (FWHM). The sample orientation was optimized for the crystallite with largest volume. Longitudinal scans at the (2 0 0) and (0 0 3) Bragg peaks gave  $\Delta q_h = 0.026$  and  $\Delta q_l = 0.045$  r.l.u. FWHM, respectively.

Before searching for the magnetic inelastic response, we measured the neutron groups corresponding to the transverse acoustic (TA) phonons propagating along [0 0 1] to determine the lowest possible vibrational excitation energy at the magnetic zone center ( $h k l + 1/2$ ). Constant-Q scans were performed around the (2 0 1/2) reciprocal lattice position with the sample kept at  $T = 10$  K. The results obtained are shown in Fig. 1. The observed energies and intensities are in good agreement with the results reported for UCoGa<sub>5</sub> [10]. In particular, the intensity at (2 0 0.7) is very weak in all cases. Since the TA[0 0 1] phonon branch reaches an energy of 7.2 meV at the magnetic zone center, any excitation with energy smaller than this value cannot be of phononic origin.

Having established the energy of the lowest vibrational excitations, we looked for the magnetic response at the (1 0 1/2) reciprocal lattice point. At this position, the intensity of the TA phonon is expected to be weaker than

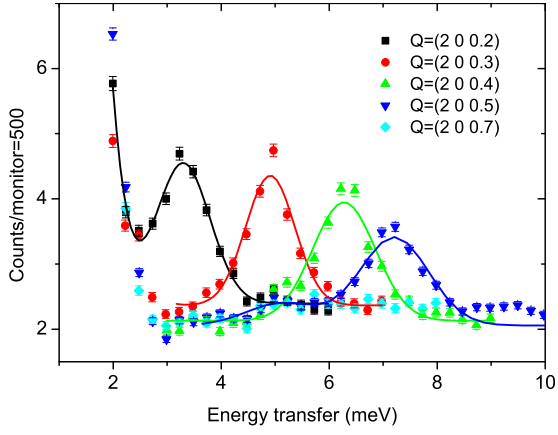


FIG. 1: Neutron groups observed with the sample at 10 K in constant-Q measurements at different wave vectors  $(2\ 0\ q_z)$ . The observed excitations correspond to TA phonons propagating along the  $[0\ 0\ 1]$  direction.

at  $(2\ 0\ 1/2)$  by almost an order of magnitude, because of the geometric factor appearing in the neutron cross-section. The results obtained are shown in Fig. 2. Data were taken as constant-Q scans at different  $Q = (1\ 0\ q_z)$  positions, and fitted to two Gaussian line-shapes. One Gaussian curve represents the contribution of the TA phonon; it is centered at the energy shown in Fig. 1 for the corresponding peak. The intensity scales with the square of the neutron momentum transfer, as expected. The second Gaussian curve is attributed to a propagating magnetic excitation, with an energy gap of  $5.5 \pm 0.2$  meV. Moving away from the magnetic zone center  $(1\ 0\ 1/2)$ , the energy of phonons decreases whereas the energy of the magnetic peak increases.

In addition, a weaker non-dispersive signal is observed at about 10.5 meV, which we attribute to a mean field excitation between crystal field (CF) levels. Due to its non dispersive behavior, this excitation is also visible in the scan performed at a generic reciprocal lattice position  $(0.8\ 0\ 1.2)$ , as shown in Fig. 2.

Equivalent scans at  $(2\ 0\ 1/2)$  and  $(3\ 0\ 1/2)$  establish an increase in the phonon contribution only, and confirm the magnetic origin of both, the propagating and the local excitation.

To better characterize the non-local magnetic response, we followed its temperature dependence by performing constant-Q scans at the  $(0\ 0\ 3/2)$  reciprocal lattice point (Fig. 3). At this position, the TA phonon contribution is minimized and the longitudinal acoustic (LA) phonon is expected at higher energies only. In addition, at such a small momentum transfer, all phononic signals are weak. The scan at the AFM zone center is compared with a scan at  $Q = (0.2\ 0\ 1.47)$ , which was reached by a  $\Theta = 12.5$  degrees sample rotation away from the optimal value for the  $(0\ 0\ 3/2)$  position. This position might be considered to reflect the Q-independent background (see

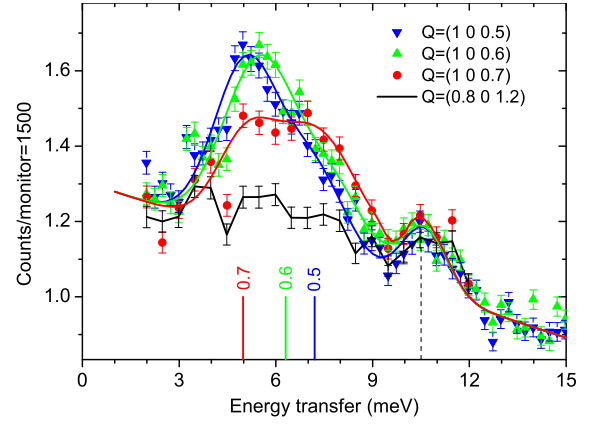


FIG. 2: Neutron groups corresponding to excitations propagating along  $[0\ 0\ 1]$  at 10 K. The solid lines are fits to the sum of two Gaussians and a sloping background, measured at  $Q = (0.8\ 0\ 1.2)$ . The third peak at 10.5 meV (dashed vertical line) is attributed to a local, non dispersive excitation. The vertical tags indicate the energy of the TA phonons, and are labelled by the corresponding  $q_z$  value.

discussion below). By subtracting the background from the intensity at the AFM zone center and dividing by the Bose factor, we obtain the temperature dependence of the imaginary component of the dynamical susceptibility (Fig. 3 b). A phonon contribution is visible at  $8.4 \pm 0.6$  meV and, as expected after Bose factor normalization, its intensity is temperature independent. On the other hand the magnetic intensity at 5.5 meV becomes weaker as the temperature increases (inset Fig.3), but it is still clearly visible above the Néel temperature,  $T_N$ . The large difference between the intensities measured at  $(0\ 0\ 1.5)$  and  $(0.2\ 0\ 1.47)$  confirms that this signal cannot be attributed to a crystal field excitation, neither below nor above the Néel temperature  $T_N$ . Indeed, the intensity of a crystal field excitation would change only as the square of the magnetic form factor, which is essentially the same at the two positions.

It is interesting to compare the static and dynamic magnetic intensities at both the  $(1\ 0\ 1/2)$  and the  $(0\ 0\ 3/2)$  positions. The static magnetic moment points along the tetragonal c-axis, and therefore all Bragg reflections of  $(0\ 0\ L)$ -type have zero neutron intensity. Since the inelastic magnetic intensity at 5.5 meV of both reflections is comparable, we suspect the dynamic fluctuations to show an (at least) significant transverse component.

Fig.4 shows longitudinal Q-scans around  $Q = (0\ 0\ q_z)$  and transverse Q-scans around  $Q = (q_x\ 0\ 3/2)$ , with neutron energy-transfer fixed at 5.5 meV. The non-local character of the 5.5 meV excitation at  $T = 10$  K is confirmed by the strong Q dependence of the intensity, which peaks at the magnetic zone center. The peaks at  $(0\ 0\ 2.85)$  and (very much weaker) at  $(0\ 0\ 1.15)$  are due to the nearby LA phonon. At this stage of our investigations, with a relaxed instrumental momentum resolu-

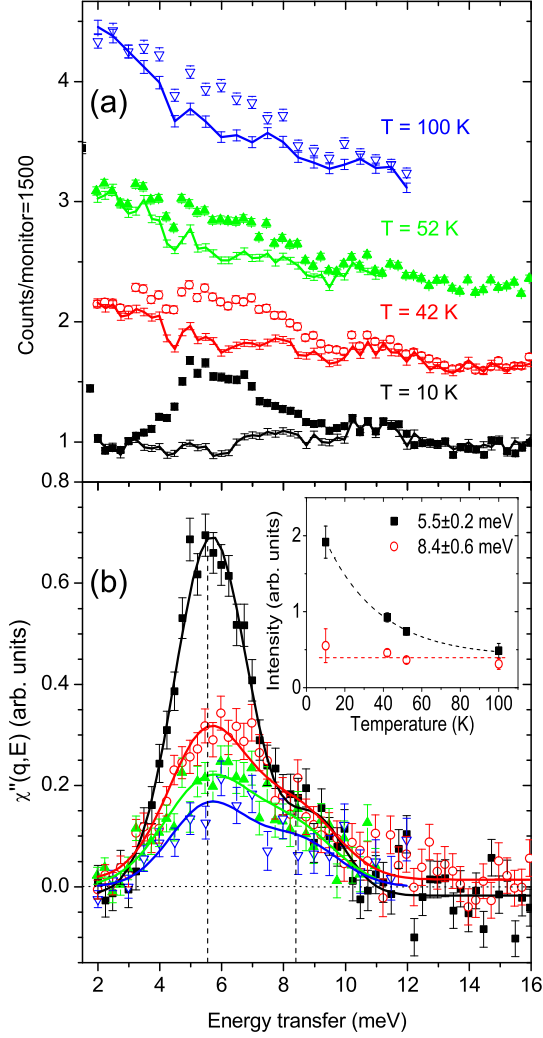


FIG. 3: (a) Constant-Q scans at different temperatures at the  $Q = (0\ 0\ 3/2)$ . A constant vertical offset of 1000 counts is applied for clarity. The solid lines are scans at  $Q = (0.2\ 0\ 1.47)$ . (b) Imaginary component of the dynamical magnetic susceptibility: squares 10 K, open circles 42 K, up triangles 52 K, down open triangles 100 K. The solid lines are fit to two Gaussian line-shapes centered at  $5.5 \pm 0.2$  and  $8.4 \pm 0.6$  meV (vertical dashed lines), with intensities shown in the inset.

tion and without polarized neutrons, we cannot establish the origin of the large background signal, which increases with temperature. This prevents any quantitative analysis of the peak width and therefore the spatial coherence length of the dispersive magnetic excitation. We note, however, that at 10 K the magnetic peak has a width comparable to that of the LA phonon, suggesting a long-range character. Approaching  $T_N$ , the magnetic response becomes much broader in  $Q$ , and only a short-range in-plane correlation appear to survive. Polarization analysis experiments are planned to address this point.

Fig. 5 shows the dispersion relation along  $[0\ 0\ 1]$  of

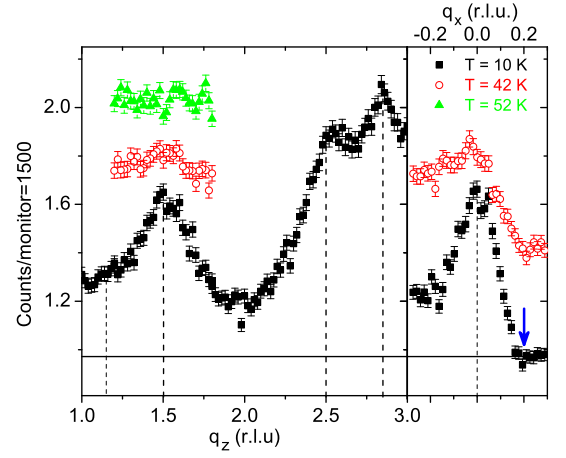


FIG. 4: Q scans at constant energy transfer,  $\hbar\omega = 5.5$  meV. Left panel: longitudinal scan along the  $[001]$  direction,  $Q = (0\ 0\ q_z)$ . Right panel: transverse scan around  $(q_x\ 0\ 1.5)$ , performed by  $\Theta$  rotation of the sample. Neutron intensity is plotted as a function of  $q_x$ . The arrow indicates the position corresponding to the scan at  $Q = (0.2\ 0\ 1.47)$  in Fig. 3. A vertical offset of 0.2 counts/monitor is applied for clarity to data at different temperature.

the excitation modes observed at 10 K in this experiment. The TA phonon dispersion falls in between the dispersion curves reported for the Pu and U homologous compounds [10, 11]. Also the point measured for the LA phonon is in good agreement with previous studies of the vibrational response in  $\text{UCoGa}_5$  and  $\text{PuCoGa}_5$ . The dispersion of the low-energy magnetic mode is typical of a spin-wave excitation in an antiferromagnet. The non-dispersive local excitation at 10.5 meV is also shown.

Previous studies [12] assume the 5f electrons to be essentially localized and predict a crystal field (CF) level at about 8 meV in the paramagnetic phase, directly coupled with a doublet ground state. On this basis, an Ising mean field (MF) model has been proposed to describe the magnetically ordered phase [13]. The Hamiltonian can be written as the sum of a CF term,

$$H_{CF} = B_2^0 O_2^0 + B_4^0 O_4^0 + B_6^0 O_6^0 + B_4^4 O_4^4 + B_6^4 O_6^4 \quad (1)$$

a nearest-neighbors exchange interaction within the  $a$ - $b$  planes,

$$H_{ab} = -\frac{1}{4} \Lambda_z \sum_{\langle ij \rangle} J_{z,i}^{(l)} J_{z,j}^{(l)} \quad (2)$$

and an interlayer exchange term

$$H_c = \frac{1}{2} \Lambda_z^\perp \sum_l J_{z,i}^{(l)} J_{z,i}^{(l+1)}, \quad (3)$$

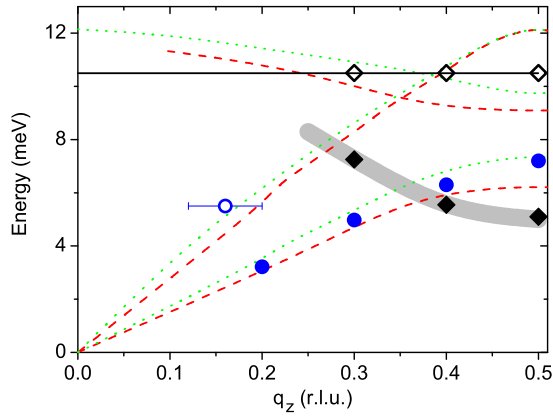


FIG. 5: Dispersion relation along  $[0\ 0\ 1]$  for the TA phonon (full circles), the LA phonon (open circle), and the two magnetic modes (full and open diamonds). Data taken at  $T = 10$  K. Dashed and dotted lines are phonon dispersion curves reported for  $\text{PuCoGa}_5$  and  $\text{UCoGa}_5$ , respectively [10, 11].

where  $O_k^q$  are Stevens operator equivalents,  $B_k^q$  the CF parameters,  $\Lambda_z$  and  $\Lambda_z^\perp$  are the intralayer and interlayer exchange constants, respectively,  $i, j$  label the Np site in the  $a$ - $b$  plane, and  $l$  indexes the layers.

Following Aoki et al. [12], the lowest lying CF eigenstates have the form

$$\begin{aligned} |d_\pm\rangle &= a|\pm 3\rangle + \sqrt{1-a^2}|\mp 1\rangle \\ |s\rangle &= c(|+4\rangle + |-4\rangle) + \sqrt{1-2c^2}|0\rangle. \end{aligned} \quad (4)$$

The doublet  $|d_\pm\rangle$  and the singlet  $|s\rangle$  are separated by a gap  $\Delta_{CF}$ , whilst the remaining states of the  $^5I_4$  multiplet have much higher energies and do not affect the low temperature properties. The exchange Hamiltonian is treated in MF approximation and the self-consistent solution is sought. The coefficient  $a$  is fixed by the value of the ordered moment, and the sum  $\Lambda_z + \Lambda_z^\perp$  is varied in order to fix  $T_N$  to the experimental value. A non-dispersive INS transition at 10.5 meV is indeed allowed if  $\Delta_{CF} = 6$  meV. This bare CF gap is close to the value proposed in [12] to explain the bulk properties in the paramagnetic phase. In the ordered phase, the doublet would be split by  $\Delta_{ex} = 9$  meV, however the corresponding INS transition would not be dipole-allowed. Therefore, within this model, the dispersive excitation appearing at 5.5 meV at the magnetic zone center cannot be understood. Its observation indicates that a fully localized dipolar model fails to describe the dynamical magnetic response of  $\text{NpCoGa}_5$ .

In conclusion, our inelastic neutron scattering experiment gives evidence for the existence of two energy scales for the magnetic excitations in the ordered phase of  $\text{NpCoGa}_5$ . One is related to a non-dispersive excitation between two crystal field levels (with a bare gap

modified by mean-field exchange), and a lower one corresponds to dispersive spin fluctuations. The CF splitting is compatible with earlier predictions based on essentially localized dipolar models, which reproduce the bulk magnetic properties in the paramagnetic phase [12]. The dispersive magnetic response, on the other hand, reveals the presence of non-local excitations with an energy gap very close to that deduced from the low temperature dependence of the specific heat [8].

As shown in Fig. 3, an inelastic magnetic response is visible also at 52 and 100 K. This signal cannot be attributed to a CF transition, because of the different intensities measured at  $Q = (0\ 0\ 3/2)$  and at  $Q = (0.2\ 0\ 1.47)$ . Therefore, although broader and weaker, the low energy excitation resulting from the spin-spin temporal correlation clearly persists in the paramagnetic phase. This supports the possibility that magnetic fluctuations centered around  $(0\ 0\ 1/2)$  are present, as suggested by theory [6], also in  $\text{PuCoGa}_5$ , where they have been proposed as a possible mediating boson responsible for the appearance of superconductivity [14].

Finally, it appears that the  $5f$  electrons in  $\text{NpCoGa}_5$  are neither completely localized nor itinerant. This dual nature is typical of the  $5f$  shell in intermetallic compounds and its elucidation is one of the main current topics in the physics of strongly correlated electron systems. Recent Mössbauer spectroscopy studies of  $\text{NpTGA}_5$  point to a tendency towards localization of the  $5f$  states with increasing number of  $d$  electrons on the transition metal  $T$  [15]. It will therefore be interesting to extend our INS investigation to  $\text{NpFeGa}_5$ , where an essentially itinerant response is expected, and to  $\text{NpNiGa}_5$ , where the localized dynamics should dominate.

- 
- [1] J. L. Sarrao and J. D. Thompson, J. Phys. Soc. Jpn. **76**, 051013 (2007).
  - [2] J. L. Sarrao, et al., Nature (London) **420**, 297 (2002).
  - [3] I. Opahle and P. M. Oppeneer, Phys. Rev. Lett. **90**, 157001 (2003).
  - [4] T. Maehira, et al., Phys. Rev. Lett. **90**, 207007 (2003).
  - [5] A. B. Shick, et al., Phys. Rev. Lett. **94**, 016401 (2005).
  - [6] L. V. Pourovskii, et al., Phys. Rev. B **73**, 060506(R) (2006).
  - [7] N. J. Curro, et al., Nature (London) **434**, 622 (2005).
  - [8] E. Colineau, et al., Phys. Rev. B **69**, 184411 (2004).
  - [9] N. Metoki, et al., Phys. Rev. B **72**, 014460 (2005).
  - [10] N. Metoki, et al., Physica B **378-380**, 1003 (2006).
  - [11] S. Raymond, et al., Phys. Rev. Lett. **96**, 237003 (2006).
  - [12] D. Aoki, et al., J. Phys. Soc. Jpn. **73**, 1665 (2004).
  - [13] A. Kiss and Y. Kuramoto, J. Phys. Soc. Jpn. **75**, 034709 (2006).
  - [14] Y. Bang, et al., Phys. Rev. B **70**, 104512 (2004).
  - [15] E. Colineau, et al., J. Phys.: Condens. Matter **19**, 246202 (2007).